The crystallographic texture of graphite-like and diamond-like boron nitride bulk materials

V. L. SOLOZHENKO*, I. A. PETRUSHA
Institute for Superhard Materials of the National Academy of Sciences of Ukraine, Kiev 254074, Ukraine
E-mail: vls@uni-bonn.de.

O. ENGLER, J. F. BINGERT
Materials Science and Technology Division, Los Alamos National Laboratory, Los Alamos, NM 87545, USA

X-ray powder diffraction and quantitative texture analysis have been employed to study the crystallographic relation of parent and product phases in direct transformations of graphite-like BN polymorphs into diamond-like BN phases at a pressure of 7.7 GPa and temperatures up to 2600 K. It has been found that the transformation of both CVD-produced bulk slightly textured turbostratic BN (tBN) and highly textured graphite-like hexagonal BN (hBN) results in a preferred orientation of the crystallites of the new cubic BN (cBN) due to the $(111)_{cBN} \parallel (001)_{tBN, hBN}$ epitaxial relation. Phase transformation of a CVD-produced bulk highly textured rhombohedral BN (rBN) results in the formation of highly textured wurtzitic BN (wBN) according to the $(100)_{wBN} \parallel (001)_{rBN}$ crystallographic relation.
© *2001 Kluwer Academic Publishers*

1. Introduction

In recent years, diamond-like phases of boron nitride—cubic (cBN) and wurtzitic (wBN)—have found a wide range of applications in tools for cutting and polishing of ferrous metals and high-temperature alloys. One of the most promising aspects of materials based on diamond-like BN phases is associated with the possibility of forming highly oriented structures. The anisotropy of mechanical properties of such textured materials might be successfully used in advanced cutting tools [1], and materials having pronounced axial textures might exhibit piezoelectric properties [2].

Such textured materials can be produced through an oriented transformation of graphite-like hexagonal (hBN) and rhombohedral (rBN) boron nitride under high pressures and temperatures. According to Kurdyumov *et al.* [3], BN diamond-like tetrahedral structures can be produced from graphite-like structures via relatively simple co-operative lattice transformations, namely, by high pressure-induced compression of the initial lattice along the hexagonal axis and a splitting of the hexagon layers by buckling or puckering. Among all phase transformations, the characteristics of the hBN–to–wBN martensitic transformation proceeding without formation of any intermediate structures are understood most comprehensively [4], and it was found that the wBN formed in this way is related to the original hBN through an orientation relationship $(001)_{wBN} \parallel (001)_{hBN}$. Under shock-wave compression of highly textured rBN, a direct rBN–to–cBN transfor-

mation accompanied by the $(111)_{cBN} \parallel (001)_{rBN}$ mutual orientation of the phases was observed [5, 6].

It should be noted that martensitic phase transformations are characteristic of highly ordered structures. Therefore, it is to be expected that in highly textured initial materials the regular orientation relationships of the phases during the martensitic transformation should result in the formation of highly textured material on the basis of BN diamond-like polymorphs. This paper presents the results of the first texture analysis performed on oriented diamond-like BN phases that were synthesised by direct conversion of CVD-produced bulk highly textured graphite-like BN at a pressure of 7.7 GPa and temperatures up to 2600 K.

2. Experimental
2.1. Samples

In the present investigation three types of graphite-like BN bulk materials were analysed: (1) CVD turbostratic boron nitride (tBN) with a density of 1.99 g/cm^3 and a three-dimensional ordering degree $P_3 = 0$ (the degree of three-dimensional ordering P_3 of graphite-like structures is defined as the ratio of regularly oriented layers to the total number of layers in the coherent scattering region); (2) CVD rhombohedral boron nitride (rBN) with a density of 2.26 g/cm^3 and $P_3 = 0.85$; (3) hexagonal graphite-like boron nitride (hBN) of theoretical density (2.279 g/cm^3) and with a perfectly ordered structure ($P_3 = 1$) that was produced
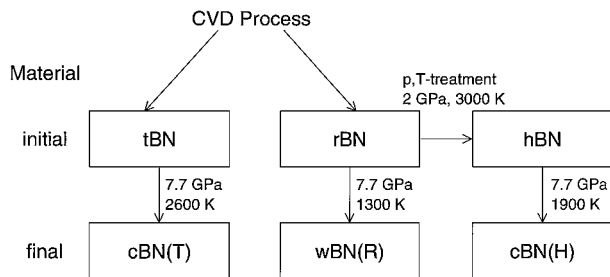

Figure 1 Schematic diagram illustrating the sample treatment.

by the rBN–to–hBN phase transformation at 2 GPa and 3000 K. A schematic diagram illustrating the various routes of sample processing is given in Fig. 1.

According to mass-spectroscopy, the total amount of metallic, carbon and oxygen impurities of the BN samples did not exceed 0.05 wt%.

For the high-pressure experiments, discs 4 mm in diameter and 0.5–0.6 mm thick were prepared. The discs were cut from CVD as-deposited plates such that the surface of the disc corresponded to the plane of deposition of the pyrolytic material.

2.2. High-pressure experiments
The high pressure experiments were carried out in a belt-type high-pressure apparatus with a hole 12.7 mm in diameter, which could be heated up to temperatures of 2100 K. Experiments at higher temperatures were performed using a toroid-type high-pressure apparatus. The experimental set-up is described in detail elsewhere [7]. The pressure within a sample during a given experiment was estimated from the force applied. For that purpose, the set-up was calibrated with the known phase transitions in bismuth and barium, *viz.* Bi_{I-II} (at 2.54 GPa), Ba_{II-III} (at 5.5 GPa) and Bi_{VI-VII} (at 7.7 GPa) at room temperature. Temperature calibration was performed using a Pt/Pt-10% Rh thermocouple without correction for the pressure effect on the electromotive force of a thermocouple. At a given pressure, the samples were heated in steps of 150 K up to the desired temperatures, with a subsequent isothermal holding time of 300 s. After the p,T-treatment the samples were quenched by switching off the heating current and releasing the pressure.

2.3. X-ray diffraction
X-ray diffraction patterns were taken in the back-reflection mode from plane surfaces of polycrystalline samples using a D-5000 SIEMENS diffractometer (Cu K_α-radiation, $\lambda = 0.154187$ nm). The diffraction patterns were scanned in steps of 0.02° in 2θ, and the reflected intensity was recorded for 10 s at each step. A high purity silicon standard was used to adjust the goniometer. The diffraction patterns were processed using the software package DIFFRAC-AT, v.3.0. The content of hexagonal and rhombohedral phases of two-phase graphite-like materials was estimated from the ratio between the intensities of the *100* hBN and *101* rBN diffraction lines. The microstructures of similar BN samples have been studied by transmission elec-

tron microscopy (TEM); the results can be found in Ref. 6.

2.4. Texture analysis
The orientation relations between the initial layered graphite-like BN phases and the final diamond-like BN polymorphs were derived from the crystallographic textures of bulk samples before and after the p,T-treatment. Texture measurements were performed in back-reflection mode with Cu K_α radiation by means of a standard X-ray texture goniometer [8]. Incomplete pole figures with radial angles $0° \leq \alpha \leq 80°$ were recorded from a sample surface normal to the compression axis of the initial material. The reflected pole figure intensities require corrections for background irradiation and the defocusing error. The background intensity was determined by measuring a pole figure about 2–3° outside the corresponding Bragg diffraction peak. In order to correct the data with respect to the defocusing error, the intensity loss with increasing tilting angle α was derived from one of the BN-samples that fortuitously had a near-random texture. It is interesting to note that for the very small sample sizes the intensity loss with increasing α— and hence the necessary corrections— were in fact *smaller* than for regular sized samples. This is attributed to the fact that even for highly tilted positions the very small samples were still largely covered by the X-ray beam (e.g. [8]). Finally, the experimental pole figures were normalised and represented by plotting iso-intensity lines in stereographic projection.

It has to be noted that the small sample size (discs with diameter of 4 mm) rendered a fully quantitative correction of the pole figures more difficult. In particular, the intensities of the outer pole circles may be subject to quite large errors. In order to assess the quality of the corrections applied, and so to substantiate the quantitative information of the pole figure analysis, from a number of pole figures of a given sample the three-dimensional orientation distribution function (ODF) was calculated. For the cubic cBN, the hexagonal hBN and the rhombohedral rBN several, typically four, pole figures could be measured and were used to compute the ODF according to the series expansion method [9]. Finally, the corresponding pole figures were recalculated. Compared to evaluating the experimental pole figures, this method offers several advantages. (i) Since the information of several pole figures with different reflection geometries is utilised, the ODF and, consequently, the recalculated pole figures embody a more reliable, averaged presentation of the "real" orientation distribution. (ii) ODFs can be calculated from incomplete pole figures with maximum tilting angles of only say $\alpha = 60°$ or 70°. This means that the ODF only contains the information of the pole figure regions in which the corrections are less critical, but, nonetheless, complete pole figures can be displayed.

Comparison of the recalculated pole figures with the corresponding experimental ones revealed no major differences between both. The recalculated pole figures tended to be smoother, which reflects the averaging effect by using several pole figures. Nonetheless, the comparison proved that the applied corrections were
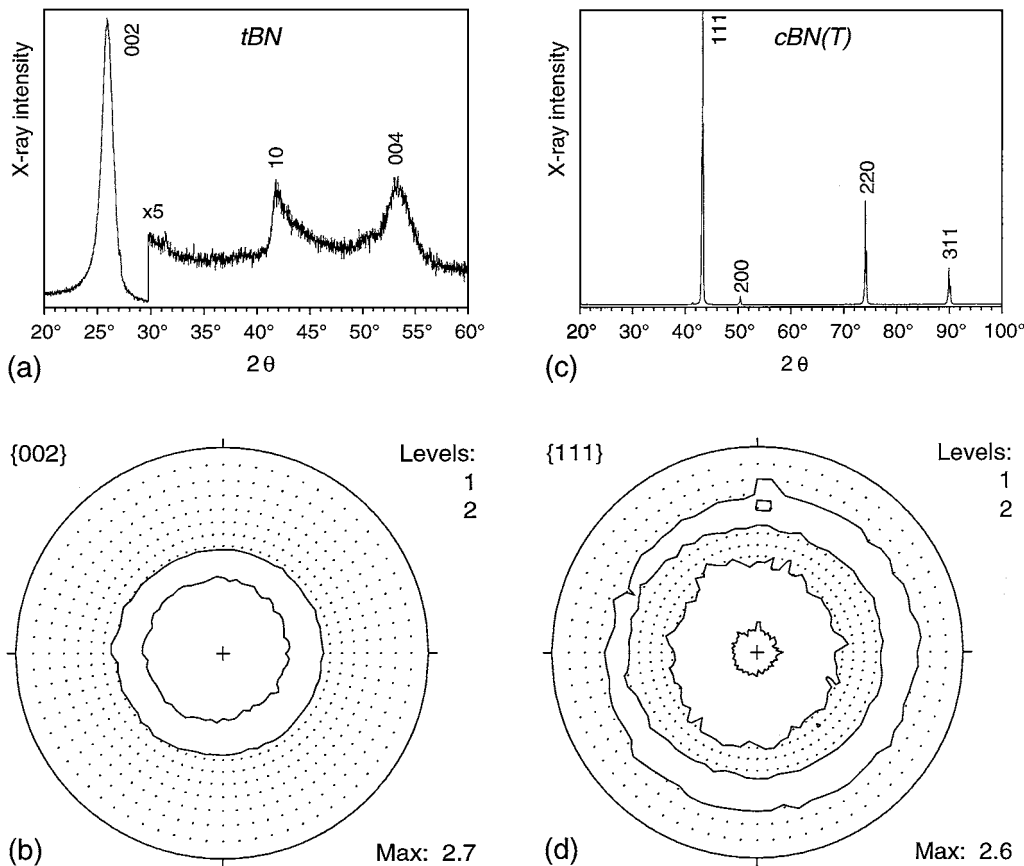
Figure 2 X-ray analysis of the tBN sample before and after phase transformation: (a) diffraction pattern of the initial tBN; (b) {002} pole figure of the initial tBN; (c) diffraction pattern of the as-synthesised cBN(T); (d) {111} pole figure of the as-synthesised cBN(T).

adequate so as to derive reliable pole figure data. For the purpose of the present investigation, experimental and recalculated pole figures are interchangeable.

3. Results and discussion
3.1. Turbostratic boron nitride (tBN)

Due to a high concentration of turbostratic stacking faults, the tBN structure is close to the ultimate structure of graphite-like boron nitride having complete one-dimensional disordering [10]. This results in the absence of the *hkl* lines with $l \neq 0$ in the diffraction pattern (Fig. 2a). In addition, this material exhibits a layer spacing of 3.44 Å, which is much higher than that of highly ordered hBN (3.3281 Å) [11] and, according to TEM-data, has a quasi-crystalline structure with the size of the disoriented elements in the basal plane being 10 nm and less [6]. The pole figure for reflection from the (002) planes is shown in Fig. 2b. According to this pole figure, the initial tBN has a very weak texture with a minor concentration of the {002} orientations in the pole figure centre. This means there is a slight preference of the {002} poles to arrange themselves normal to the sample surface. In the azimuthal plane of the sample, that is, in the directions perpendicular to the direction of the material deposition, no preferred orientations were obtained. Thus, it is assumed that the sample has a weak {002} fibre texture with a random orientation of the crystallites in the azimuthal plane, although no further pole figures of the tBN phase could be measured to confirm this point.

At a pressure of 7.7 GPa, tBN undergoes no structural transformations up to temperatures approaching 2600 K, at which point a phase transformation into cubic boron nitride is observed without any intermediate phases. The resulting material is composed of single-phase cBN(T) crystallites*, whose sizes, according to TEM examinations, vary from fractions of a micrometer up to a few micrometers. The material is characterised by a very weak {111} fibre texture, as indicated by one {111} axis being parallel to the sample normal and the others forming an axisymmetric distribution approximately 70° about the former (Fig. 2d). Considering the weak {002} fibre texture in the initial material (Fig. 2b), it can be concluded that the new phase forms through an oriented nucleation; the crystallographic orientation relation between the tBN and cBN crystal lattices can be written as $(111)_{cBN} \parallel (001)_{tBN}$.

3.2. Rhombohedral BN (rBN)

TEM investigations have shown that the initial rBN material is coarse-grained with particle sizes of up to several tens of micrometers [6]. The structure of the material is characterised by a high density of defects, as confirmed by the TEM contrast. Selected area diffraction (SAD) displayed continuous diffuse streaks of the *0kl* reflections, which is indicative of a high concentration of stacking faults. X-ray diffraction

---

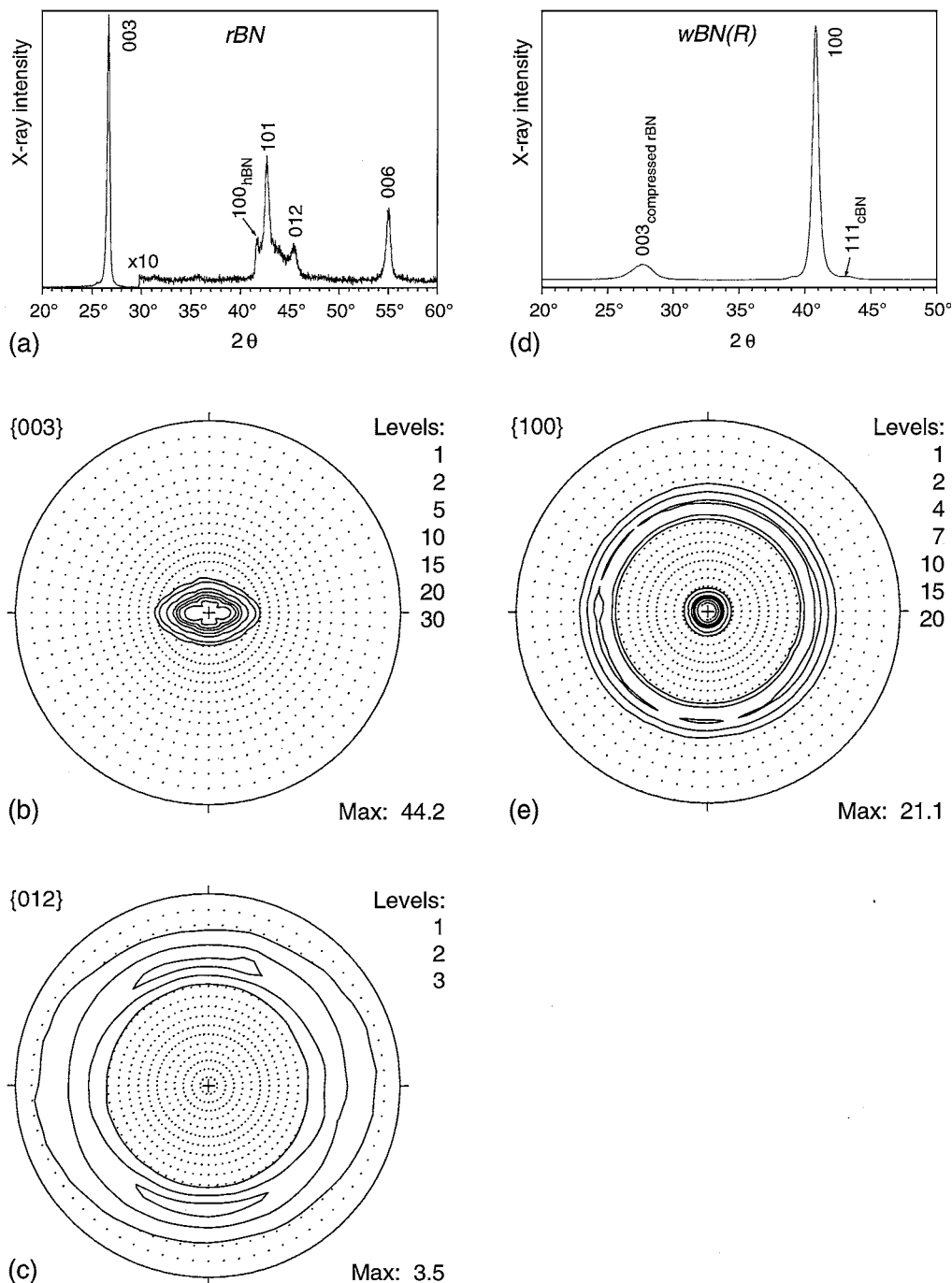* The suffix (T) indicates that the resulting cBN was synthesised from tBN, etc.

Figure 3 X-ray analysis of the rBN sample before and after phase transformation: (a) diffraction pattern of the initial rBN; (b) {003} pole figure of the initial rBN; (c) {012} pole figure of the initial rBN; (d) diffraction pattern of the as-synthesised wBN(R); (e) {100} pole figure of the as-synthesised wBN(R).

revealed that the material contained up to 10 vol% disordered hBN (Fig. 3a). The {003} pole figure of the initial material points to a very high degree of texturing (Fig. 3b). The material is comprised of a strong {001} fibre texture with the fibre axis approximately parallel to the sample normal. In the azimuthal plane the crystallites were randomly oriented, which is confirmed by analysing the {012} pole figure (Fig. 3c), which revealed uniformly distributed intensities under ~66° to the pole figure centre.

At a pressure of 7.7 GPa the formation of wBN is observed starting at room temperature. The degree of the rBN–to–wBN transformation considerably increased at temperatures above 500 K; at 1300 K the wBN content

of the sample exceeded 85 vol%. The structure of the resulting wBN(R) featured a highly preferred orientation of crystallites (Fig. 3d and e). The texture analysis showed that the orientation relationship between the new phase wBN(R) and the initial rBN corresponds to a $(100)_{wBN} \parallel (001)_{rBN}$ crystallographic relation, which means that the phase transformation proceeds via the base-prism mechanism [6]. Due to the very sharp {100} fibre texture there is not a sufficient number of grains with other orientations, so that the X-ray diffraction pattern taken from the disc surface (Fig. 3d) exhibits only the intense *100* line of wBN. Furthermore, a weak, broad line was observed at 3.204 Å that was interpreted as the *003* line of unconverted highly compressed

graphite-like BN. The very weak line corresponding to a layer spacing of 2.09 Å is probably associated with a small amount of cBN in the sample.

The crystallographic mechanism of the rBN–to–wBN transformation suggests the formation of different intermediate structures because of the different possible types of deformation of the parent graphite-like structure during transformation (either uniform shear in the basal plane [6] or microtwinning [12]). According to Kurdyumov *et al.* [6], at low temperatures deformation primarily occurs through shears in the basal plane accompanied by grain fragmentation. Above 500 K, intensive twinning of rBN along the (101) planes was observed. These characteristics of the rBN deforma-

tion define two alternative mechanisms of the rBN–to–wBN transformation. First, a shear deformation along the basal planes facilitates the formation of an intermediate structure with a stacking sequence ADAD and the splitting of hexagon layers by the buckling hexagon scheme, for which the following orientation relations of crystal lattices of the parent and forming phases occur:

$$(100)_{wBN}\|(001)_{i\text{-m ADAD}}\|(001)_{rBN};$$

$$[10\bar{1}0]_{wBN}\|[0001]_{i\text{-m ADAD}}\|[0001]_{rBN} \quad (1)$$

Second, twinning facilitates a direct transformation by a mechanism proposed recently by Britun [12]. In this case the following orientation relation is observed:
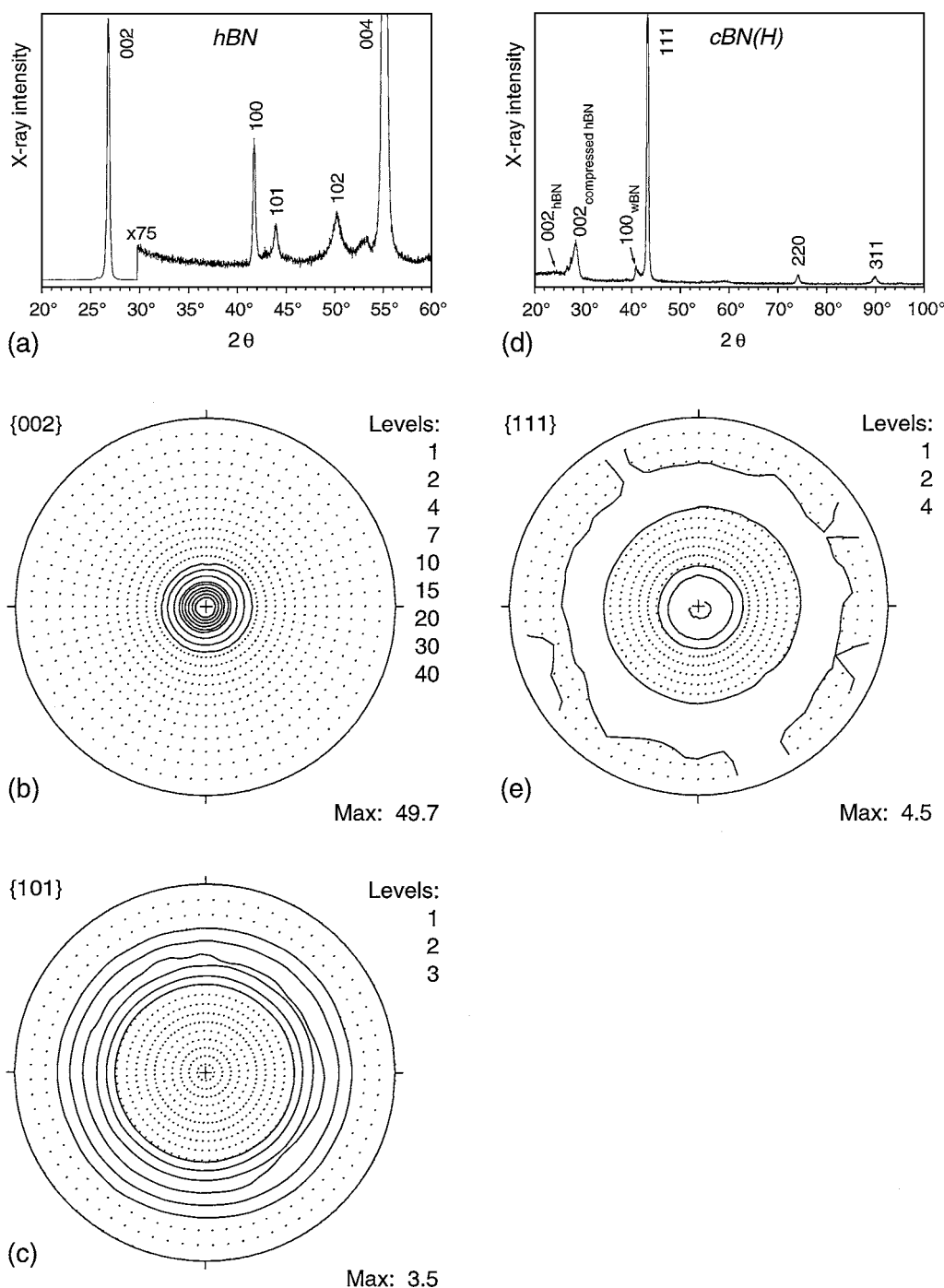

Figure 4 X-ray analysis of the hBN sample before and after phase transformation: (a) diffraction pattern of the initial hBN; (b) {002} pole figure of the initial hBN; (c) {101} pole figure of the initial hBN; (d) diffraction pattern of the as-synthesised cBN(H); (e) {111} pole figure of the as-synthesised cBN(H).

$$(001)_{wBN} \| (101)_{rBN}; \quad [10\bar{1}0]_{wBN} \| [3034]_{rBN} \quad (2)$$

This arises from a preliminary twinning along the (101) rBN planes that then reconstruct into the (001) planes of the wurtzitic phase. In both cases the (100) planes of the forming wBN are mainly oriented parallel to the (001) planes of the parent rBN. Thus, the phase transformations by both of the above mechanisms should result in the $(100)_{wBN} \| (001)_{rBN}$ orientation relation, and it is precisely this relation that is observed experimentally.

According to this crystallographic relation, one of the prismatic planes {100} of each wBN crystallite is oriented parallel to the (001) basal plane of the initial rBN material, which gives rise to the central pole in the pole figure (Fig. 3e). The other, crystallographically equivalent prismatic planes form an axisymmetric ring with more or less evenly distributed intensities near 60° in the pole figure (Fig. 3e). This means that the crystallites of the wurtzitic phase are randomly oriented in the azimuthal plane parallel to the sample surface, which is attributed to the absence of preferred orientations of the crystallites in the azimuthal plane of the initial pyrolytic rBN material (Fig. 3c).

3.3. Hexagonal boron nitride (hBN)

The initial hBN(R) material revealed a high degree of texturing with a sharp {002} fibre texture (Fig. 4a, b and c). The $(001)_{hBN} \| (001)_{rBN}$ orientation relation, corresponding to the experimentally observed texture relation $\{0001\}_{hBN} \| \{0001\}_{rBN}$, is the natural crystallographic relation for the rBN–to–hBN phase transition by which the hBN(R) sample has been produced (Fig. 1, see Fig. 3b and c).

At 7.7 GPa and temperatures above 1300 K the formation of cBN from the bulk hBN was observed. At 1900 K, the cBN content of the sample exceeded 85–90 vol%. The X-ray diffraction pattern of the cBN(H) sample exhibited a sharp *111* line of the cubic phase (Fig. 4d), which is due to the preferred orientation of cBN crystallites with (111) planes parallel to the sample surface (Fig. 4e). The sample contained a small amount of unconverted graphite-like phase both in a highly compressed ($d = 3.14$ Å) and a "normal" ($d = 3.331$ Å) state. The line corresponding to the layer spacing of 2.207 Å is due to the reflection from the (100) planes of a textured wurtzitic phase. This phase can form by one of the two mechanisms (1) and (2) described earlier from rBN impurities that exist in the initial material hBN(R) because of an incomplete rBN–to–hBN phase transformation during the sample preparation. The most interesting experimental fact is the observed $\{111\}_{cBN} \| \{001\}_{hBN}$ texture relation that corresponds to the crystallographic relation $(111)_{cBN} \| (001)_{hBN}$ between the parent and the final phase. The obtained cBN(H) polycrystalline material has a rather weak {111} fibre texture (Fig. 4e). The high level of cBN imperfection and the relatively low temperature of its formation suggest a co-operative nature of the hBN-to-cBN transformation in this particular case.

The crystallographic mechanism of this transformation can not be explained in terms of the simple shear deformations of the hBN lattice. A reconstruction of bonds, which is required because of the different periodicity of the atomic packing in hBN and cBN, seems to be difficult to achieve since the transformation occurred in a temperature range where self-diffusion processes in boron nitride are not significant. A probable transformation mechanism that would account for the observed $\{111\}_{cBN} \| \{001\}_{hBN}$ orientation relation between the parent and the new phase is a two-step mechanism via an intermediate wBN phase. In the first step the parent hBN transforms to wBN by the martensitic mechanism of puckering basal layers [6]. In this step, the orientations of the new phase are related to the original phase through the orientation relationship $(001)_{wBN} \| (001)_{hBN}$. In the second step the wBN phase transforms into the final cBN through the formation of multilayer polytypes as intermediate structures. In this case, the orientation relation is $(111)_{cBN} \| (001)_{wBN}$ because of the epitaxial homology between both the close packed planes of these phases and the (001) planes of the multilayer polytypes.

4. Conclusions

We have studied the crystallographic relation of parent graphite-like BN polymorphs and diamond-like BN structures that form by phase transformations at a pressure of 7.7 GPa and temperatures up to 2600 K. Our findings allow the following conclusions about the occurrence of preferred crystallographic orientations and orientation relations between parent and transformed phases.

Polycrystalline structures of cBN form by transformations of both weakly textured tBN and highly textured hBN. In both cases the orientation relation of the newly formed cBN phase with respect to the parent phase is $(111)_{cBN} \| (001)_{tBN, hBN}$. The degree of texturing of the final cBN phase depends on that of the parent graphite-like BN material.

During structural and phase transformations of highly textured rBN, wBN forms, whose structure features another type of a highly preferred orientation of crystallites. The texture studies show that the mutual orientation relation of the two phases corresponds to a $(100)_{wBN} \| (001)_{rBN}$ crystallographic relation. This means that the phase transformation occurs by the base–prism mechanism.

References

1. T. NISHIGUCHI and M. MASUDA, in Proc. 14th North American Manufacturing Research Conf. (NAMRI) (Dearborn, MI, 1986) p. 459.
2. H.-C. HWANG, *Phys. Rev*. B **17** (1978) 4100.
3. A. V. KURDYUMOV and N. F. OSTROVSKAYA, *Fizika i Tekhnika Vysokikh Davlenii* **2** (1992) 5 (in Russian).
4. A. V. KURDYUMOV, *Soviet Physics—Doklady* **20** (1975) 218.
5. T. SATO, T. ISHII and N. SETAKA, *J. Amer. Ceram. Soc.* **65** (1982) 162.
6. A. V. KURDYUMOV, V. F. BRITUN and I. A. PETRUSHA, *Diamond and Related Mater.* **5** (1996) 1229.
7. V. L. SOLOZHENKO, I. A. PETRUSHA and B. BARBIER, *J. Superhard Mater.* **18** (1996) 55.
8. V. RANDLE and O. ENGLER, "Introduction to Texture Analysis: Macrotexture, Microtexture and Orientation Mapping" (Gordon and Breach Science Publ., 2000).
9. M. DAHMS and H. J. BUNGE, *J. Appl. Cryst.* **22** (1989) 439.
10. A. V. KURDYUMOV, V. G. MALOGOLOVETS, N. V. NOVIKOV, A. N. PILYANKEVICH and L. A. SHULMAN, "Polymorphic Modifications of Carbon and Boron Nitride" (Metallurgiya, Moscow, 1994) (in Russian) p. 318.
11. A. V. KURDYUMOV, V. L. SOLOZHENKO and W. B. ZELYAVSKI, *J. Appl. Cryst.* **28** (1995) 540.
12. V. F. BRITUN, *J. Superhard Mater.* **14** (1992) 1.